Original research

Advancing genotype-phenotype analysis through 3D facial morphometry: insights from Cri-du-Chat syndrome

Michiel Vanneste ,[1,2] Harold Matthews ,[1,2] Yoeri Sleyp,[1] Peter Hammond,[1] Mark Shriver,[3] Seth M Weinberg,[4,5] Mary L Marazita,[4,5] Susan Walsh,[6] Benedikt Hallgrimsson,[7,8,9] Ophir D Klein,[10] Richard Spritz,[11] Kris Van Den Bogaert,[12] Peter Claes,[1,2,13] Hilde Peeters[1,12]

► Additional supplemental material is published online only. To view, please visit the journal online (https://doi.org/10.1136/jmg-2025-110940).

For numbered affiliations see end of article.

Correspondence to
Professor Hilde Peeters;
hilde.peeters@kuleuven.be

Received 20 May 2025
Accepted 8 October 2025
Published Online First 20 November 2025

ABSTRACT

Purpose Facial dysmorphism is a feature of many monogenic disorders and is important in diagnostics, variant interpretation and nosology. Nevertheless, comprehensively assessing the complex facial shape changes associated with specific syndromes remains challenging. Here, we present three-dimensional (3D) morphometric approaches to overcome these limitations, using Cri-du-Chat syndrome (CdCS) as a model.

Methods We analysed 3D facial images from 24 participants with CdCS, 4540 unaffected controls and five participants with rare 5p15.33-15.32 deletions, incorporating two methods to account for age- and sex-related facial variation. We quantified phenotypic variation within and between groups and explored genotype-phenotype correlations in CdCS.

Results We identified changes in the characteristic facial features of CdCS with age and found that facial shape in CdCS differed from controls in highly consistent directions, but with varying magnitudes of effect. 5p15.33-15.32 heterozygotes had non-specific dysmorphic features that were objectively different from those in CdCS, delineating multiple critical regions for facial dysmorphism on chromosome 5p.

Conclusion This work explores 3D facial morphometry to complement the standard clinical assessment of facial dysmorphism. It provides insights into the genetic basis of facial shape in CdCS and highlights the potential of 3D morphometric techniques to facilitate clinical diagnostics, variant interpretation and delineation of syndrome nosology.

WHAT IS ALREADY KNOWN ON THIS TOPIC

⇒ Facial dysmorphism is a core feature of Cri-du-Chat syndrome (CdCS), but the contributions of different regions on 5p to facial dysmorphism in CdCS remain unclear.

WHAT THIS STUDY ADDS

⇒ Using three-dimensional (3D) morphometric tools, we objectively assess facial dysmorphism in CdCS and delineate multiple critical regions for facial dysmorphism on chromosome 5p.

HOW THIS STUDY MIGHT AFFECT RESEARCH, PRACTICE OR POLICY

⇒ This work demonstrates that 3D facial morphometry enables an objective, quantitative assessment of facial features that is complementary to the traditional qualitative clinical assessment.

INTRODUCTION

Facial dysmorphism exists in many monogenic disorders, and accurate assessment of dysmorphic features contributes to diagnostics, nosology and variant interpretation.[1 2] While standardised terminology facilitates consistent reporting of dysmorphic features by clinicians worldwide,[3] it remains challenging to capture the complex three-dimensional (3D) facial phenotype associated with specific disorders using this lexicon.[4] Furthermore, facial shape is influenced by factors such as age, sex and genetic ancestry, which complicate evaluating facial dysmorphism and assessing phenotypic variation.[1 5] This study applies 3D morphometric techniques to address these limitations, using Cri-du-Chat syndrome (CdCS; MIM: 123450) as a model.

CdCS is a contiguous gene deletion disorder resulting from heterozygous deletions on chromosome 5p, with an incidence of 1/15 000 to 1/50 000 live births.[6 7] There are no recurring breakpoints and deletion sizes range from 500 kb to 45 Mb. However, most affected individuals carry terminal deletions of 10 Mb or larger involving the 5p15.31 and 5p15.2 regions.[6 8–10] Typical clinical features of CdCS include global developmental delay, delayed speech development, microcephaly, a high-pitched cat-like cry in infancy and facial dysmorphism.[6 11] CdCS demonstrates considerable phenotypic variability, in part attributed to differences in deletion size and breakpoints.[6 12] Recurring facial features include hypertelorism, epicanthic folds, a prominent nasal bridge, short philtrum, microcephaly and micrognathia; nevertheless, a recognisable facial gestalt is not always present.

Despite the lack of recurring breakpoints, some genotype-phenotype correlations have been established (figure 1). The degree of intellectual disability (ID) is associated with the deletion size and position, with usually moderate ID in individuals with deletions limited to 5p15.2 and severe ID in individuals with larger deletions or concurrent chromosomal abnormalities.[6 8 10 11] Similarly, 5p15.32 deletions

To cite: Vanneste M, Matthews H, Sleyp Y, *et al*. *J Med Genet* 2026;**63**:95–102.

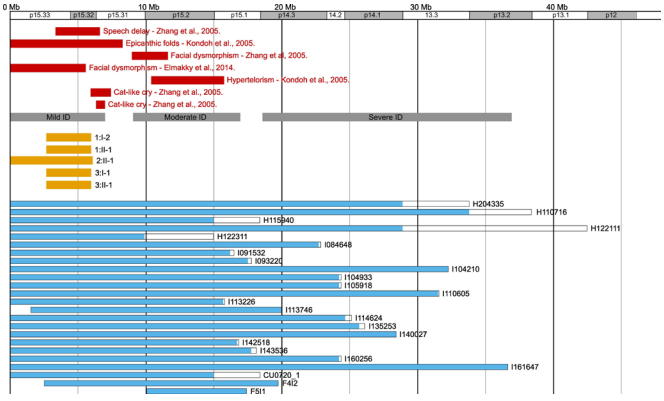

Figure 1 Map of chromosome 5p. Map of chromosome 5p with cytogenetic bands displayed at the top. In red, the previously reported critical regions for different phenotypic characteristics of Cri-du-Chat syndrome (CdCS); in grey, the genotype-phenotype correlations for intellectual disability (ID) and in yellow, the deleted regions of the 5p15.33-15.32deletion heterozygotes. Blue bars represent the minimal size of the deletions in the CdCS reference cohort, the white areas correspond to the maximal size (ie, last present array probe).

are linked to speech delay[10] and deletions of 5p15.31 appear to be critical for the cat-like cry.[10 13] For facial dysmorphism, however, there is conflicting evidence about which regions are critical. Various overlapping and non-overlapping deletions have been reported in individuals with varying facial features, and the specific contributions of the corresponding chromosomal regions to facial dysmorphism in CdCS thus remain unclear.[9–12]

Recently, efforts towards a more objective evaluation of facial dysmorphism have given rise to next-generation phenotyping tools. Advances in morphometric analysis have facilitated the development of tools that objectively match two-dimensional (2D) and 3D photographs to known syndromic gestalts and suggest syndromic diagnoses.[14 15] Open-source 3D craniofacial growth curves enable age-adjusted and sex-adjusted assessments of facial morphology,[16] and a model to quantify phenotypic variation was published.[1] Together, these advances enable a quantitative, objective assessment of facial dysmorphism.

We used these next-generation 3D phenotyping tools to study facial dysmorphism in CdCS. We quantified the phenotypic variation in CdCS, delineated the recurring facial features and investigated changes in facial phenotype with age. We also studied the facial dysmorphism in five individuals with small 5p15.33-15.32 deletions and objectively compared it with participants with larger 5p deletions, delineating critical regions for typical and atypical facial dysmorphism in CdCS.

MATERIALS AND METHODS

Sample composition

We compiled a CdCS reference cohort from 3D facial images, demographic data (self-reported age, sex and ancestry) and molecular testing results of 98 participants with a clinical and/or molecular diagnosis of CdCS from three sources. We obtained previously collected data on 59 participants with CdCS from the online FaceBase repository (FB00000861 (https://doi.org/10.25550/TJ0[17])) and 37 from Peter Hammond's legacy 3D dysmorphology dataset hosted at KU Leuven. Two participants previously diagnosed with CdCS at the Centre for Human Genetics of University Hospitals Leuven were recontacted for inclusion in this study. We only included participants with available molecular testing results (n=34) and further excluded participants with poor image quality (n=3), incomplete metadata (n=1) and additional pathogenic genetic variants besides a 5p deletion (n=1). Because we relied on 3D facial growth curves limited to individuals of European ancestry,[16] we necessarily excluded participants of self-reported non-European ancestry (n=4) to retain a curated CdCS cohort of 24 participants (online supplemental data 1). Genotypes were determined by different cytogenetic techniques with different resolutions (conventional karyotyping, bacterial artificial chromosome comparative genomic hybridisation array (Agilent) and 180k chromosomal microarray analysis (CMA) (Oxford Gene Technologies)). All genotype data, including regions of uncertainty due to resolution differences, were mapped to GRCh38 genomic locations using LiftOver, developed by the University of California, Santa Cruz (https://genome.ucsc.edu/cgi-bin/hgLiftOver)[18] and Ensembl (Release 109)[19] (figure 1, online supplemental data 1).

We also collected 3D facial images and clinical data of five participants with heterozygous 5p15.33-15.32 deletions from three families. All deletions were previously identified through CMA in a clinical workup at University Hospital Gasthuisberg (Leuven, Belgium).

We used a large control sample (n=4680) of previously collected 3D facial images and demographic data (age, sex, self-reported ancestry) from the 3D Facial Norms cohort[20] and studies at the Pennsylvania State University and Indiana University-Purdue University Indianapolis. We excluded participants with ages outside the 3D craniofacial growth curves age range (females: 0.5–68.9 years; males: 0.5–51.8 years), retaining 4540 participants. Sex and age distribution of this sample is provided in online supplemental figure 1 and online supplemental data 2; sample characteristics and participant recruitment have been described in detail by White *et al*.[21]

3D image acquisition and processing

3D facial images were acquired using digital stereophotogrammetry systems (3dMDface, Vectra H1) with submillimetric accuracy.[22] We non-rigidly registered an average facial template to each image using the MeshMonk toolbox (V.0.0.6)[23] to obtain a standardised facial representation defined by 7160 homologous quasi-landmarks. The deformed template corresponds anatomically across all images and facilitates meaningful comparison between images, regardless of pre-processing differences in facial position.[24]

Growth curves and facial signatures

We calculated facial signatures to measure local shape deviation compared with a normative reference.[25] Per participant, we compared all quasi-landmarks to an age-matched and sex-matched normative reference, determined using open-source 3D craniofacial growth curves.[16] We calculated facial signatures as z-scores for local shape deviation along three Cartesian axes (x-, y- and z-signatures) and, for visualisation purposes, locally perpendicular to the facial surface. Since the control sample was previously included to construct the growth curves, we calculated their facial signatures using a modified approach, comparing each participant's facial shape with a variation model constructed on the entire sample, excluding their own facial shape. To distinguish between facial shape differences affecting the full face or parts of the face, we performed the assessments described below twice; once including all quasi-landmarks (full face) and once including only the quasi-landmarks of the midface (online supplemental figure 2).

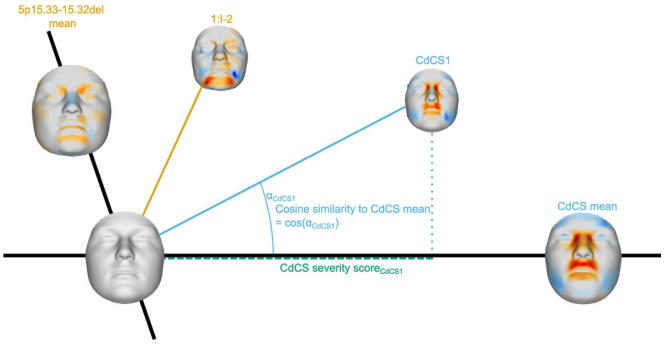

Figure 2 Quantifying phenotypic variation: cosine similarity and severity score. Two-dimensional representation of the multidimensional 'face space' used to quantify phenotypic variation. The mean facial signature of the Cri-du-Chat syndrome (CdCS) cohort and 5p15.33-15.32 deletion (5p15.33-15.32del) heterozygotes is shown, as well as their corresponding feature vectors (black bold lines). The facial shape and signature of a participant of each group (orange=5p15.33-15.32del; blue=CdCS) are displayed. As illustrated for participant CdCS1, the cosine similarity to the CdCS mean is calculated based on the angle α between the individual and mean CdCS feature vectors, providing a value between −1 and 1 that represents the multivariate correlation between the directions of the individual and mean feature vectors. The CdCS severity score is calculated by projecting the individual vector on the mean feature vectors (blue dotted line), measuring the magnitude of the projected vector along the phenotype axis of interest (green dotted line).

Quantifying phenotypic variation through facial signatures

We assessed phenotypic variation within and between groups following the methodology outlined by Matthews *et al*.[1] We concatenated facial signatures in the x-, y- and z-directions, followed by dimensionality reduction using singular value decomposition. This way, each participant's face is represented by a single feature vector in a high-dimensional 'feature vector space' and facial signature similarity is reflected by proximity in that space.[26] We calculated a mean feature vector for each diagnostic group (CdCS cohort, 5p15.33-15.32 deletion and controls), representing its average facial signature.

The phenotypic similarity between two (individual or mean) facial signatures was then calculated as the cosine similarity ($\cos(\alpha)$, where α is the angle between the corresponding feature vectors; figure 2). The cosine similarity ranges from −1 to 1, indicating two feature vectors have exactly opposite or identical directions, respectively (thus representing a multivariate correlation between two facial signatures). We measured phenotypic severity as the projection of a participant's feature vector onto the group mean, yielding a 'severity score' (figure 2). We performed pairwise comparisons of the cosine similarities with the CdCS mean and CdCS severity scores across groups using two-sample Kolmogorov-Smirnov tests (kstest2, Matlab R2024b).

We quantified within-group phenotypic variation using two metrics: 'directional variation' and 'severity variation'. Directional variation measures the variation in direction of individual feature vectors and was computed as the root mean square of 1− cosine similarity to the group mean. Severity variation measures the variation in magnitude of individual feature vectors along a specific direction and was computed as the standard deviation of the severity scores. Throughout these calculations, we used a leave-one-out approach, where the participant being scored is excluded from the group mean. Variation magnitudes were compared with previously published values from 39 monogenic disorders with facial dysmorphism.[1]

Statistical shape analysis through covariate-adjusted principal component analysis

We performed principal component analysis (PCA) to assess phenotypic similarity independent from the cosine similarity analysis. We aligned the control facial shapes using generalised Procrustes analysis and adjusted for sex, age and age-squared using partial least squares regression (PLSR). We then Procrustes superimposed the CdCS shapes onto the control mean and adjusted for covariates using the PLSR coefficients from the control model. The aligned and covariate-adjusted shapes were then subjected to PCA in three different designs. We performed PCAs on the CdCS cohort (CdCS-PCA) and control sample (control-PCA) separately to assess within-group variation, and assessed between-group variation through a joint PCA of the CdCS cohort and an age-matched and sex-matched control subset (matched-PCA, online supplemental data 3) that was randomly selected from the larger control sample without replacement. Lastly, we projected the facial shapes of the 5p15.33-15.32 deletion heterozygotes into the matched-PCA space to evaluate similarity-based clustering. For all PCAs, we used a 98% cumulative variance explained cut-off.

Effect of age, sex and deletion size

To investigate associations between facial shape and age or deletion size in the CdCS cohort, we performed linear regressions (fitlm, Matlab R2024b) using age and deletion size as predictors and CdCS severity scores, cosine similarities to the CdCS mean and covariate-adjusted CdCS-PCA scores as response variables. P values were Bonferroni corrected. To validate the covariate adjustment in the CdCS cohort, we applied it to 100 matched control sets (n=24), selecting sex-matched and age-matched controls from the larger sample without reselecting participants. Facial shapes were aligned and adjusted for sex, age and age-squared using PLSR coefficients from the remaining controls (n=4516) and then subjected to PCA. We found no significant associations between age and PCA scores postadjustment (online supplemental figure 3, online supplemental data 4).

RESULTS

Cohort description

We assembled a CdCS reference cohort of 24 participants with heterozygous 5p deletions (figure 1). Twenty-one deletions were terminal and three were interstitial, ranging from 7 to 42 Mb (online supplemental data 1). All deletions encompassed 5p15.2, which was previously reported as critical for the ID and facial dysmorphism of CdCS (figure 1).[10 12] In addition to this reference cohort, we included five participants from three families with smaller heterozygous 5p15.33-15.32 deletions of 3.3 Mb or 6.0 Mb (figures 1 and 3). Molecular karyotyping in these families was initially performed because of facial dysmorphism and motor delay (participant 1:II-1) or developmental delay (participants 2:II-1 and 3:II-1). Clinical and molecular summaries are shown in table 1, detailed clinical data are provided in online supplemental data 5.

Facial signatures reliably assess individual and recurring dysmorphic features

Clinical assessment of the CdCS reference cohort showed that all participants had some facial features typical for CdCS, such as short philtrum (24/24; 100%), prominent nasal bridge (21/24; 88%), epicanthic folds (20/24; 83%), micrognathia (17/24; 71%) and hypertelorism (12/24; 50%) (figure 4A, online supplemental data 1). Only seven participants (29%) showed all five

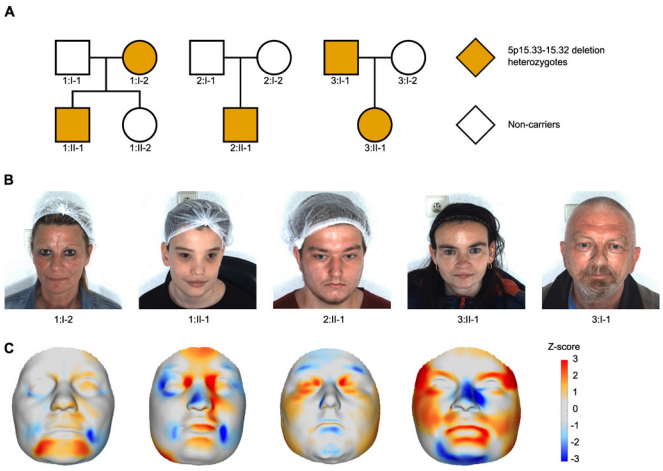

Figure 3 5p15.33-15.32 deletion heterozygotes. (A) Pedigrees of the 5p15.33-15.32 deletion heterozygotes. (B) Facial photographs of the five 5p15.33-15.32 deletion heterozygotes. All participants gave permission for publication of these pictures. (C) Facial signatures of the five 5p15.33-15.32 deletion heterozygotes. The colours correspond to the degree of local shape deviation (in z-scores compared with an age-matched and sex-matched normative reference) locally perpendicular to the surface (blue=inward displacement, red=outward displacement). For participant 3:I-1, no facial signature was calculated, as their images did not pass quality control due to their beard.

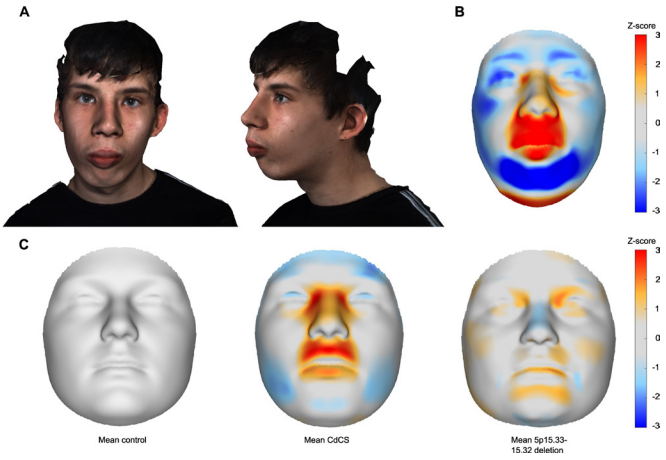

Figure 4 Facial dysmorphism in CdCS. (A) Participant from the Cri-du-Chat syndrome (CdCS) cohort with typical facial features of CdCS, including a prominent nasal bridge, short philtrum, hypertelorism and micrognathia. Written informed consent for recognisable publication was provided. (B) Facial signature of the same participant, highlighting how their facial shape deviates from an age-matched normative face. Red indicates outward deviation locally perpendicular to the surface, blue indicates inward deviation. (C) Mean facial shapes and signatures for the control sample, CdCS reference cohort and 5p15.33-15.32del heterozygotes.

features, while 18 (75%) had at least four. Clinically, two participants (8%; I161647 and I091532) lacked the typical CdCS facial gestalt. Both had the characteristic short philtrum and one had epicanthic folds, but both also had coarser facial features without prominent nasal bridge, micrognathia or hypertelorism (online supplemental figure 4, online supplemental data 1).

We calculated facial signatures for the CdCS cohort to perform an objective assessment of facial shape (figure 4B). Individually, facial signatures highlight how a participant's facial shape deviates from an age-matched and sex-matched normative face (figure 4A–B). Concordance was high between the facial signatures and the clinical assessment for the nasal bridge and philtrum, with lower concordance for micrognathia (online supplemental data 1). In three participants, micrognathia was clinically subtle but clear in the facial signature, while in another three, a clinical impression of micrognathia was not confirmed by the facial signature. Evaluating the concordance was not possible for epicanthic folds and hypertelorism, as these features cannot be distinguished from each other on a facial signature. The CdCS mean facial signature (figure 4C) showed a short philtrum, prominent nasal bridge, triangular facial shape with micrognathia and a strong signal at the inner canthi consistent with epicanthic folds and/or hypertelorism. In contrast, the control mean facial signature (n=4540) showed no recurring features (figure 4C). These findings align with the clinical assessment and previous reports,[6 11] demonstrating the utility of facial signatures in visualising recurring facial features in a cohort.

Cosine similarity provides quantitative assessment of between-group variation

To quantify facial differences between the CdCS cohort and controls, we used two metrics derived from facial signatures: cosine similarity and severity score. The cosine similarity reflects the similarity in direction of facial deviation of two faces, while the severity score measures the magnitude of that deviation along a specific phenotype axis (figure 2). Participants with CdCS showed significantly higher cosine similarities to the CdCS mean than controls for both the full face and the midface ($p=4.0\times10^{-15}$ and $p=1.1\times10^{-11}$, respectively; two-sample Kolmogorov-Smirnov test), indicating their facial phenotypes were consistently different from controls (figure 5A,B, online supplemental data 6). CdCS cosine similarities and severity scores were not associated with deletion size or age (online supplemental figure 5). A PCA of CdCS and matched controls (matched-PCA) confirmed these findings. PC1 and PC2 were

Table 1 Summary of primary data for five participants with 5p15.33-15.32 deletion

Identifier	Age at inclusion (years)	Sex	High pitched voice as infant	DD	Microcephaly	Speech delay	Molecular results (GRCh38 breakpoints) and inheritance
1:I-2	47.8	Female	Unknown	No	No	No	46, XX, del 5p15.33-5p15.32 (NC_000005.10:g.2682860_5982650del), inheritance unknown
1:II-1	12.5	Male	Yes	Motor delay*	No	No	46, XY, del 5p15.33-5p15.32 (NC_000005.10:g.2682860_5982650del), maternally inherited
2:II-1	19.6	Male	Yes	Mild global DD	No	No	46, XX, del 5p15.33-5p15.32 (NC_000005.10:g.16497_6093321del), de novo
3:I-1	59.5	Male	Unknown	Mild global DD	No	No	46, XY, del 5p15.33-5p15.32 (NC_000005.10:g.2682860_5982650del), inheritance unknown
3:II-1	31.3	Female	No	Yes	No	Yes	46, XX, del 5p15.33-5p15.32 (NC_000005.10:g.2682860_5982650del), paternally inherited

DD, developmental delay; ID, intellectual disability.

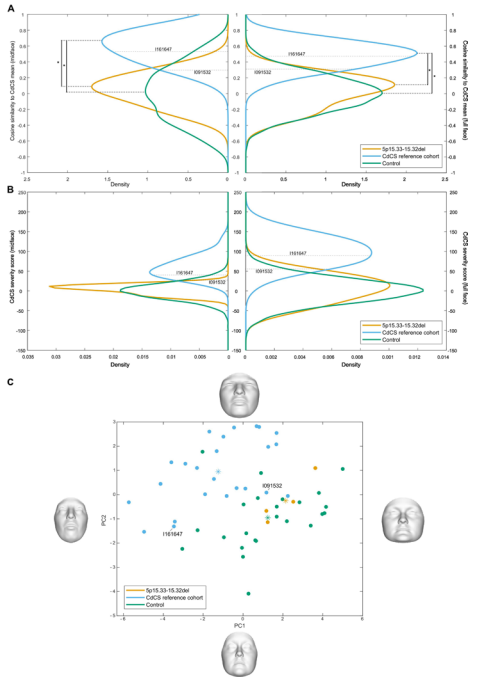

Figure 5 Between-group phenotype comparisons. Probability density functions of the cosine similarity to the Cri-du-Chat syndrome (CdCS) mean (A) and CdCS severity scores (B) for the participants of the CdCS reference cohort, controls and the 5p15.33-15.32 deletion (5p15.33-15.32del) heterozygotes, calculated on the full face (right) and midface (left). In (A), significant differences between density functions are marked with an asterisk (two-sample Kolmogorov-Smirnov test, Bonferroni correction). (C) Scatter plot of the first two principal components of the PCA on the CdCS cohort and matched controls. 5p15.33-15.32del heterozygotes were projected into the PC space, stars indicate the projected positions of the group means. The facial shapes show the facial shape at ±3 SD of the PC scores. In all panels, the scores for the two participants with a clinical outlier phenotype are indicated.

both strongly correlated with the CdCS cosine similarity and severity scores (online supplemental figure 6) and captured core clinical characteristics of CdCS such as the short philtrum, prominent nasal bridge, hypertelorism and micrognathia (figure 5, online supplemental media 1 and 2). The PC1 and PC2 scores varied considerably for the CdCS cohort, but still effectively distinguished cases from controls (figure 5C). This supports the findings of the cosine similarity analysis that the facial phenotype in CdCS is variable but consistently different from controls.

Facial signatures in CdCS have a consistent direction but variable magnitude of effect

We quantified within-group phenotypic variation using 'directional variation' and 'severity variation' metrics derived from cosine similarity and severity scores, calculated separately for the full face and midface. Directional variation quantifies differences in the pattern of how facial features covary, while severity variation describes differences in the magnitude of facial features. Full face directional variation in the CdCS cohort was in the ninth lowest percentile (0.54; 95% CI (0.45 to 0.58)) compared with other monogenic disorders.[1] The midface, which includes most of the characteristic dysmorphic features of CdCS, showed even lower directional variation (0.45; 95% CI (0.35 to 0.45)). In contrast, directional variation was significantly higher in controls (full face=1.01; 95% CI (1.00 to 1.02), midface=1.04; 95% CI (1.02 to 1.05)). Severity variation was low in both groups for the full face (CdCS severity variation=35.4; 95% CI (27.5 to 49.7), control severity variation=30.4; 95% CI (29.7 to 31.0)), scoring in the seventh and third lowest percentiles, respectively. Interestingly, midface severity variation was significantly higher in CdCS than in controls (CdCS severity variation=26.7; 95% CI (20.8 to 37.5), control severity variation=17.2; 95% CI (16.8 to 17.5)). These results suggest that facial features in CdCS are highly consistent in direction, especially in the midface, but with variable expressions of severity across participants.

The typical facial features of CdCS change with age

We performed a PCA on the CdCS facial shapes (CdCS-PCA) to investigate the primary axes of phenotypic variation within this cohort. PC1 was significantly associated with age even though the facial shapes were adjusted for general facial variation associated with age, corroborating previous reports that the facial features of CdCS change as individuals get older[8 27] (online supplemental figure 7A). The shape effects captured by PC1 (online supplemental figure 7A) showed a more prominent nasal bridge and micrognathia as participants got older, and less pronounced hypertelorism and/or epicanthic folds. The philtrum, which was consistently assessed as short in all participants in the CdCS cohort, remained largely unchanged. The same effects were present when comparing the mean facial signatures of the youngest and oldest halves of the CdCS cohort (ages 2–12 vs 15–43 years) (online supplemental figure 7C,D). A covariate-adjusted PCA of facial shape in the control sample (control-PCA) showed no significant associations with age and captured different primary axes of variation (online supplemental figure 7B), indicating that the age-associated axis of variation is specific to the CdCS cohort. Linear regression of the covariate-adjusted CdCS shapes on age also indicated a changing phenotype with age (online supplemental media 3). Interpretation is limited by the cohort's uneven age distribution, but applying these methodologies to larger or longitudinal cohorts would enable a detailed study of age-related facial changes in CdCS.

Objective analysis explains outlier phenotypes

Two CdCS participants (I091352 and I161647) lacked the typical CdCS facial gestalt on clinical assessment, and we attempted to quantify this outlier clinical impression. For both participants, the facial signatures corresponded well to the clinically described coarser facial features and the absence of a prominent nasal bridge and epicanthic folds (online supplemental figure 4A). For I091352, this was reflected in a low cosine similarity to the CdCS mean, a low CdCS severity score and close clustering to controls on the matched-PCA (figure 5A–C), confirming an atypical CdCS phenotype. In contrast, I161647 showed average cosine similarity to the CdCS mean and CdCS severity scores, suggesting a relatively typical CdCS phenotype (figure 5A–B). As the oldest participant of the CdCS cohort, their facial features were atypical for their age group (online supplemental figure 8). The clinical impression of an outlier phenotype in this participant was thus likely explained by their less prominent nasal bridge and absence of micrognathia on a background of normal age-related variation, which is an unusual combination among older individuals with CdCS.

Facial features in 5p15.33-15.32 deletion heterozygotes are different from those in typical CdCS

Finally, we compared the facial features of the 5p15.33-15.32 deletion heterozygotes with the CdCS reference

cohort, who have 'typical' deletions involving 5p15.2, to assess the contribution of these distinct 5p regions to the facial dysmorphism in CdCS. Clinically, only participant 1:II-1 had some facial features resembling typical CdCS, with hypertelorism and epicanthic folds (figure 2B). The other 5p15.33-15.32 deletion heterozygotes showed no marked facial dysmorphism and no recurring dysmorphic features. Their facial signatures (figure 2C) highlighted hypertelorism in three participants, but none showed the typical prominent nasal bridge or short philtrum. The 5p15.33-15.32 deletion mean signature suggested a shared nasion shape and a prominent chin (figure 3C), although interpretation is limited by sample size. Their cosine similarities to the CdCS mean were significantly lower than in the CdCS reference cohort ($p=0.001$, two-sample Kolmogorov-Smirnov test), and did not differ significantly from those of controls ($p=0.93$) (figure 5A). When projected into the matched-PCA space, the 5p15.33-15.32 deletion heterozygotes clustered with controls rather than with the CdCS cohort, again indicating their facial features are different from participants with typical 5p deletions.

DISCUSSION

Accurately assessing dysmorphic facial features can contribute to correct diagnosis, accurate nosology and variant interpretation in clinical genetics, yet remains challenging even for experienced dysmorphologists.[5 28] In this study, we applied 3D morphometric techniques to objectively study facial dysmorphism in CdCS. We calculated facial signatures to account for age-related and sex-related variation and found they were highly concordant with the clinical assessment on an individual level. In some younger participants, clinical impressions of micrognathia were not supported by the facial signatures. Re-evaluation confirmed its absence, suggesting prior knowledge about the diagnosis influenced the initial assessment (ie, confirmation bias). At the group level, the mean facial signature showed that the most consistent facial features of CdCS are hypertelorism, prominent nasal bridge, short philtrum and prominent upper lip. These findings align with the clinical literature,[6 9 12] and we consider the mean facial signature as a valid representation of the CdCS facial gestalt. In addition to previous reports,[1] our results illustrate that individual and mean facial signatures can objectively quantify complex syndromic shape transformations and can support clinicians in interpreting facial dysmorphism.

Quantitative assessment of phenotypic variation revealed a highly consistent direction of facial shape change in the participants with typical 5p deletions. Although this might appear contradictory to the previously reported phenotypic variability in CdCS,[6 11] it highlights the complementarity of quantitative 3D phenotyping and traditional clinical assessments. While the direction of facial shape change associated with CdCS was highly consistent, the magnitude of these changes was variable, especially in the midface. The direction of effect and effect size of a facial shape transformation are likely difficult to discern clinically, contributing to the perceived phenotypic variability in CdCS. Variation in age and sex introduces additional phenotypic variability that complicates the clinical assessment, whereas our approach corrects for these sources of variation using craniofacial growth curves. Lastly, minor qualitative features like epicanthic folds can influence a dysmorphologist's opinion in comparing patients.[28] In facial signatures, however, minor features involving few data points have less influence on the global shape transformation than shape changes involving many data points such as prominent nasal bridge or short philtrum.

We applied these tools to a male patient aged 13 years (participant 1:II-1) with motor delay, pronounced hypertelorism and epicanthic folds. Genetic testing identified a small heterozygous 5p15.33-15.32 deletion, and the dysmorphic features were clinically interpreted as consistent with typical CdCS. However, morphometric analyses of five 5p15.33-15.32 deletion heterozygotes showed no consistent dysmorphic features. Although the limited sample size warrants caution in interpretation, their facial signatures differed from typical CdCS and their cosine similarity to CdCS was as low as that of controls. This highlights a common pitfall in clinical dysmorphology, where certain features (e.g. epicanthic folds) can be overinterpreted despite the overall facial phenotype matching poorly. Overinterpretation is especially likely when facial features are reinterpreted after molecular results are known, an increasingly common scenario with genotype-first approaches.[29] 3D facial phenotyping can provide objective measures to complement the clinical art of dysmorphology, avoiding overinterpretation of either assessment through careful integration of the findings with clinical knowledge and expertise.

Previous studies were inconclusive about which chromosomal regions are critical for facial dysmorphism in CdCS.[10 12] Our findings support the presence of multiple critical regions for facial dysmorphism on chromosome 5p. Individuals with deletions limited to 5p15.33-15.32 showed heterogeneous facial dysmorphism, distinct from the typical CdCS features in individuals with deletions including 5p15.2. This suggests the existence of a region on 5p15.33-15.32 for which deletion causes atypical facial dysmorphism that can include epicanthic folds, and a second region on 5p15.2 critical for features such as ocular hypertelorism, prominent nasal bridge and short philtrum. This could explain the conflicting previously reported regions, as well as the occurrence of atypical phenotypes in individuals with small terminal or subterminal deletions.[9 10 12 30] We found no other correlations between deletion size and phenotypic severity or typicality, suggesting that facial phenotypic variation in CdCS is not driven by additional critical regions but rather by other factors such as DNA methylation and polygenic background.[31 32]

3D imaging captures more anatomical data than 2D photos and is robust to differences in lighting and position,[24] enabling detailed analyses even with limited sample sizes. This is particularly advantageous when investigating rare diseases. However, 3D morphometry still faces methodological challenges. Craniofacial growth curves have improved the reliability of 3D phenotyping,[16 33] but are currently limited to individuals of European ancestry. Second, the scarcity of 3D images of individuals with rare conditions increases the risk of ascertainment bias.[34 35] Accessible 3D facial imaging using smartphones could facilitate broad data collection across diverse populations and address these limitations.[36] Lastly, the development of user-friendly 3D morphometry software is necessary to improve accessibility to a broader audience.

Despite these challenges, previous work showed that 3D morphometric tools can assist in diagnostics and variant interpretation[33 37] and provide insights into the genetics of facial shape.[21 32 38] We applied recent advances like 3D facial growth curves and phenotypic variation metrics to identify outlier phenotypes, genotype-phenotype correlations and dissect sources of phenotypic variation. We illustrate how clinicians and researchers can combine 3D photos of individuals with rare disorders with open-source 3D morphometry tools and databases to answer key questions in clinical

genetics. 3D facial morphometry enabled an objective characterisation and interpretation of facial dysmorphism, offering a valuable complement to traditional clinical assessment and a promising tool in the era of precision medicine.

Author affiliations
[1]Department of Human Genetics, Katholieke Universiteit Leuven, Leuven, Belgium
[2]Medical Imaging Research Centre, University Hospitals Leuven, Leuven, Belgium
[3]Department of Anthropology, Penn State University, University Park, Pennsylvania, USA
[4]Center for Craniofacial and Dental Genetics, Department of Oral and Craniofacial Sciences, School of Dental Medicine, University of Pittsburgh, Pittsburgh, Pennsylvania, USA
[5]Department of Human Genetics, School of Public Health, University of Pittsburgh, Pittsburgh, Pennsylvania, USA
[6]Department of Biology, Indiana University Purdue University Indianapolis, Indianapolis, Indiana, USA
[7]Department of Cell Biology & Anatomy, University of Calgary Cumming School of Medicine, Calgary, Alberta, Canada
[8]Alberta Children's Hospital Research Institute, University of Calgary Cumming School of Medicine, Calgary, Alberta, Canada
[9]McCaig Bone and Joint Institute, University of Calgary Cumming School of Medicine, Calgary, Alberta, Canada
[10]Department of Pediatrics, Cedars-Sinai Guerin Children's, Los Angeles, California, USA
[11]Department of Pediatrics, University of Colorado Denver Anschutz Medical Campus, Aurora, Colorado, USA
[12]Center for Human Genetics, University Hospitals Leuven, Leuven, Belgium
[13]Department of Electrical Engineering, ESAT/PSI, Katholieke Universiteit Leuven, Leuven, Belgium

Contributors Conceptualisation: MV, HP; data curation: MV, HM; software: MV, HM, PC; formal analysis: MV, KVDB, HP; visualisation: MV; funding acquisition and resources: PH, MS, SMW, MLM, SW, SR, BH, ODK, RS, PC, HP; supervision: PC, HP; writing—original draft: MV, HP; writing—review and editing: MV, HM, YS, PH, MS, SMW, MLM, SW, SR, BH, ODK, RS, KV, PC, HP; guarantor: HP.

Funding This work was supported by the Research Fund KU Leuven (BOF-C1, C14/15/081 and C14/20/081 to PC and HP) and the Research Program of the Research Foundation-Flanders (FWO, G0D1923N to PC and HP). HP is a senior clinical investigator of the Research Foundation Flanders (FWO). FaceBase data collection and analyses were supported by NIH-NIDCR (U01-DE024440 to RS, ODK and BH). Pittsburgh personnel, data collection and analyses were supported by the National Institute of Dental and Craniofacial Research (U01-DE020078 to MLM and SMW; R01-DE016148 to MLM and SMW; R01-DE027023 to SMW). Funding for genotyping was supported by the National Human Genome Research Institute (X01-HG007821 and X01-HG007485 to MLM). Penn State personnel, data collection and analyses were supported by the Center for Human Evolution and Development at Penn State, the Science Foundation of Ireland Walton Fellowship (04.W4/B643 to MS), the US National Institute of Justice (2008-DN-BX-K125 to MS; 2018-DU-BX-0219 to SW) and by the US Department of Defense. IUPUI personnel, data collection and analyses were supported by the National Institute of Justice (2015-R2-CX-0023, 2014-DN-BX-K031 and 2018-DU-BX-0219 to SW).

Competing interests None declared.

Patient consent for publication Consent obtained directly from patient(s).

Ethics approval This study was approved by the Ethical Review Board of KU Leuven and University Hospitals Leuven, S65629. Participants gave informed consent to participate in the study before taking part.

Provenance and peer review Not commissioned; externally peer reviewed.

Data availability statement Data are available in a public, open access repository. Data are available on reasonable request. Data may be obtained from a third party and are not publicly available. Data sharing is not applicable as no datasets were generated and/or analysed for this study. Phenotype, genotype and demographic data of the CdCS cohort were mostly collected previously and were obtained from the online FaceBase repository (FB00000861 (https://doi.org/10.25550/TJ0)) and an in-house collection. Access to the FaceBase data requires institutional ethics approval and approval from the FaceBase data access committee. Access to the three-dimensional (3D) facial surface models of the previously existing in-house collection of participants with CdCS (n=37) is not possible because these data were previously collected without consent for broad data sharing consent. Access to the facial surface models and clinical data that were collected for this study (two participants with CdCS, five participants with a 5p15.33-15.32 deletion and their relatives) is not possible because consent for data sharing was not provided. The control sample (n=4680) was collected previously and included samples from the 3D Facial Norms cohort and studies at the Pennsylvania State University and Indiana University-Purdue University Indianapolis. The 3D facial surface models of the 3D Facial Norms cohort are available through the FaceBase Consortium (FB00000491.01 (https://doi.org/10.25550/VWP)). The participants making up the PSU and IUPUI datasets were previously collected without consent for broad data sharing. This restriction is not because of any personal or commercial interests. Additional details can be requested from MS and SW for the PSU and IUPUI datasets, respectively. The MeshMonk toolbox for mesh-to-mesh registration is publicly available at https://gitlab.kuleuven.be/mirc/meshmonk.

ORCID iDs
Michiel Vanneste https://orcid.org/0000-0003-0222-5740
Harold Matthews https://orcid.org/0000-0002-0524-0025

REFERENCES

1 Matthews H, Vanneste M, Katsura K, *et al*. Refining nosology by modelling variation among facial phenotypes: the RASopathies. *J Med Genet* 2023;60:285–93.
2 Aponte JD, Bannister JJ, Hoskens H, *et al*. An interactive atlas of three-dimensional syndromic facial morphology. *Am J Hum Genet* 2024;111:39–47.
3 Allanson JE, Biesecker LG, Carey JC, *et al*. Elements of morphology: introduction. *Am J Med Genet A* 2009;149A:2–5.
4 Mubungu G, Roelants M, Lumaka A, *et al*. Objective evaluation of facial features in Congolese newborns by facial measurements. The need for population-specific measurements. *Am J Med Genet A* 2022;188:3063–70.
5 Lumaka A, Cosemans N, Lulebo Mampasi A, *et al*. Facial dysmorphism is influenced by ethnic background of the patient and of the evaluator. *Clin Genet* 2017;92:166–71.
6 Nevado J, Bel-Fenellós C, Sandoval-Talamantes AK, *et al*. Deep Phenotyping and Genetic Characterization of a Cohort of 70 Individuals With 5p Minus Syndrome. *Front Genet* 2021;12:645595.
7 Cerruti Mainardi P. Cri du Chat syndrome. *Orphanet J Rare Dis* 2006;1:33.
8 Mainardi PC, Pastore G, Castronovo C, *et al*. The natural history of Cri du Chat Syndrome. A report from the Italian Register. *Eur J Med Genet* 2006;49:363–83.
9 Elmakky A, Carli D, Lugli L, *et al*. A three-generation family with terminal microdeletion involving 5p15.33-32 due to a whole-arm 5;15 chromosomal translocation with a steady phenotype of atypical cri du chat syndrome. *Eur J Med Genet* 2014;57:145–50.
10 Zhang X, Snijders A, Segraves R, *et al*. High-resolution mapping of genotype-phenotype relationships in cri du chat syndrome using array comparative genomic hybridization. *Am J Hum Genet* 2005;76:312–26.
11 Nguyen JM, Qualmann KJ, Okashah R, *et al*. 5p deletions: Current knowledge and future directions. *Am J Med Genet C Semin Med Genet* 2015;169:224–38.
12 Kondoh T, Shimokawa O, Harada N, *et al*. Genotype-phenotype correlation of 5p-syndrome: pitfall of diagnosis. *J Hum Genet* 2005;50:26–9.
13 Wu Q, Niebuhr E, Yang H, *et al*. Determination of the "critical region" for cat-like cry of Cri-du-chat syndrome and analysis of candidate genes by quantitative PCR. *Eur J Hum Genet* 2005;13:475–85.
14 Hsieh T-C, Bar-Haim A, Moosa S, *et al*. GestaltMatcher facilitates rare disease matching using facial phenotype descriptors. *Nat Genet* 2022;54:349–57.
15 Hallgrímsson B, Aponte JD, Katz DC, *et al*. Automated syndrome diagnosis by three-dimensional facial imaging. *Genet Med* 2020;22:1682–93.
16 Matthews HS, Palmer RL, Baynam GS, *et al*. Large-scale open-source three-dimensional growth curves for clinical facial assessment and objective description of facial dysmorphism. *Sci Rep* 2021;11:12175.
17 Hallgrimsson B, Spritz R, Ophir K, *et al*. Data from: Developing 3D Craniofacial Morphometry Data and Tools to Transform Dysmorphology. *FaceBase Consortium* 2017.
18 Raney BJ, Barber GP, Benet-Pagès A, *et al*. The UCSC Genome Browser database: 2024 update. *Nucleic Acids Res* 2024;52:D1082–8.
19 Harrison PW, Amode MR, Austine-Orimoloye O, *et al*. Ensembl 2024. *Nucleic Acids Res* 2024;52:D891–9.
20 Weinberg SM, Raffensperger ZD, Kesterke MJ, *et al*. The 3D Facial Norms Database: Part 1. A Web-Based Craniofacial Anthropometric and Image Repository for the Clinical and Research Community. *The Cleft Palate Craniofacial Journal* 2016;53:185–97.
21 White JD, Indencleef K, Naqvi S, *et al*. Insights into the genetic architecture of the human face. *Nat Genet* 2021;53:45–53.
22 White JD, Ortega-Castrillon A, Virgo C, *et al*. Sources of variation in the 3dMDface and Vectra H1 3D facial imaging systems. *Sci Rep* 2020;10:4443.

23 White JD, Ortega-Castrillón A, Matthews H, *et al*. MeshMonk: Open-source large-scale intensive 3D phenotyping. *Sci Rep* 2019;9:6085.
24 Claes P, Walters M, Clement J. Improved facial outcome assessment using a 3D anthropometric mask. *Int J Oral Maxillofac Surg* 2012;41:324–30.
25 Hammond P, Suttie M, Hennekam RC, *et al*. The face signature of fibrodysplasia ossificans progressiva. *Am J Med Genet A* 2012;158A:1368–80.
26 Ferry Q, Steinberg J, Webber C, *et al*. Diagnostically relevant facial gestalt information from ordinary photos. *Elife* 2014;3:e02020.
27 Wilkins LE, Brown JA, Nance WE, *et al*. Clinical heterogeneity in 80 home-reared children with cri du chat syndrome. *J Pediatr* 1983;102:528–33.
28 Sleyp Y, Matthews HS, Vanneste M, *et al*. Toward 3D facial analysis for recognizing Mendelian causes of autism spectrum disorder. *Clin Genet* 2024;106:603–13.
29 Wilczewski CM, Obasohan J, Paschall JE, *et al*. Genotype first: Clinical genomics research through a reverse phenotyping approach. *Am J Hum Genet* 2023;110:3–12.
30 Almeida VT, Chehimi SN, Gasparini Y, *et al*. Cri-du-Chat Syndrome: Revealing a Familial Atypical Deletion in 5p. *Mol Syndromol* 2023;13:527–36.
31 Almeida VT, Chehimi SN, Carvalho GFS, *et al*. Differences in DNA methylation status explain phenotypic variability in patients with 5p- syndrome. *BMC Res Notes* 2024;17:121.
32 Vanneste M, Hoskens H, Goovaerts S, *et al*. Syndrome-informed phenotyping identifies a polygenic background for achondroplasia-like facial variation in the general population. *Nat Commun* 2024;15:10458.
33 Hammond P, Hannes F, Suttie M, *et al*. Fine-grained facial phenotype–genotype analysis in Wolf–Hirschhorn syndrome. *Eur J Hum Genet* 2012;20:33–40.
34 Santen GWE, Clayton-Smith J. ARID1B-CSS consortium. The ARID1B phenotype: what we have learned so far. *Am J Med Genet C Semin Med Genet* 2014;166C:276–89.
35 Kline AD, Moss JF, Selicorni A, *et al*. Diagnosis and management of Cornelia de Lange syndrome: first international consensus statement. *Nat Rev Genet* 2018;19:649–66.
36 Quinzi V, Polizzi A, Ronsivalle V, *et al*. Facial Scanning Accuracy with Stereophotogrammetry and Smartphone Technology in Children: A Systematic Review. *Children (Basel)* 2022;9:1390.
37 Mahdi SS, Matthews H, Nauwelaers N, *et al*. Multi-Scale Part-Based Syndrome Classification of 3D Facial Images. *IEEE Access* 2022;10:23450–62.
38 Hoskens H, Liu D, Naqvi S, *et al*. 3D facial phenotyping by biometric sibling matching used in contemporary genomic methodologies. *PLoS Genet* 2021;17:e1009528.